PRESSURE EVOLUTION FROM HEAD-ON REFLECTION OF HIGH-SPEED DEFLAGRATION IN HYDROGEN MIXTURES

Yang, H. X.[a], Wang, W. T. [b], Sow, A. [a]and Radulescu, M. I.[a]

[a]Dept. of Mechanical Engineering, University of Ottawa, 161 Louis-Pasteur St., Ottawa, ON, Canada

[b]Ford Motor Company of Canada, 700 Palladium Dr, Kanata, ON K2V 1C9, Canada

ABSTRACT

Our previous reported experiments revealed that the reflection of high-speed deflagrations in hydrogen-air and hydrogen-oxygen mixtures produces higher mechanical loading and reflected pressures than reflecting detonations. This surprising result was shown to correlate with the onset of detonation in the gases behind the reflected shock. We revisit these experiments with the aim of developing a closed-form model for the pressure evolution due to the shock-induced ignition and rapid transition to detonation. We find that the reflection condition of fast deflagrations corresponds to the chain-branching cross-over regime of hydrogen ignition, in which the reduced activation energy is very large and the reaction characteristic time is very short compared to the induction time. We formulate a closed-form model in the limit of fast reaction times as compared to the induction time, which is used to predict a square wave pressure profile generated by self-similar propagation of internal Chapman-Jouguet detonation waves followed by Taylor expansion waves. The model predictions are compared with Navier-Stokes numerical simulations with full chemistry, as well as simple Euler calculations using calibrated one-step, or two-step chain-branching models. Both simplified numerical models were found to be in good agreement with the full chemistry model. We thus demonstrate that the end pressure evolution due to the reflection of high-speed deflagrations can be well predicted analytically and numerically using relatively simple models in this ignition regime of main interest for safety analysis and explosion mitigations. The slight departures from the square wave model are investigated based on the physical wave processes occurring in the shocked gases, controlling the shock-to-detonation transition. Using the two-step model, we study how the variations of the rate of energy release control the pressure evolution in the end gas, extending the analysis of Sharpe to very large rates of energy release.

1 INTRODUCTION

The reflected pressure and impulse generated by high-speed combustion waves reflecting normal to a wall are of importance in explosion safety. Depending on the mixture sensitivity, there is a continuous spectrum of wave speeds of high-speed deflagrations, quasi-detonations and detonations, ranging from close to the sound speed of the combustion product all the way to the Chapman-Jouguet (CJ) detonation speed. The over-pressures generated by these waves range from 10 up to 35 times the initial pressure. Recently, we have observed that the highest over-pressures were achieved when the incident wave was a high-speed deflagration lead by a shock [1, 2]. They were followed, in order of importance by the reflected pressure generated by quasi-detonations, detonations, shock-flame complexes with mild ignition, and shock-flame without re-ignition. Visualization of the reflection dynamics revealed that the high mechanical loads generated by reflecting high speed deflagrations were due to rapid formation of detonation waves immediately after reflection. In the present study, we wish to model these events and establish the mechanisms controlling the level of mechanical loads.

The problem of shock induced ignition and transition to detonation has a long history, since Strehlow and coworkers first showed experimentally the sequence of events leading to detonation formation [3]. Theoretical effort in understanding these dynamics adopted mostly simplified chemical models. Extensive numerical and theoretical efforts have been made to model the flow field caused by the shock-induced ignition using simplified one-step irreversible Arrhenius kinetic - see for example [4] and references

therein. A physically more realistic model for hydrogen ignition is a two-step combustion model mimicking the chain branching character of the ignition dynamics [5]. This model has individual control of the induction and reaction zone. It has been found that a qualitatively different result may be obtained using chain-branching chemistry models than found for one-step chemistry [5]. The two-step model, when fitted to data from homogeneous explosion calculations, can give very good agreement with full reaction kinetics of hydrogen mixtures [6].

In the present study, we wish to develop an analytical model for predicting the pressure evolution in the end gas following the reflection of a high speed deflagration. We focus on the experimental conditions reported previously [2] for reflected high speed deflagrations generated by passing a detonation across a perforated plate. In the following, we will demonstrate that the reflected shocks due to high speed deflagrations bring the gas to the most sensitive state, which is near the chain-branching cross-over limit. The very large activation energies and ratios of induction to reaction times in this regime permits us to formulate a very simple analytical model for the pressure evolution, extending the analysis of Sharpe for a two step model to very large rates of energy addition. The model prediction is compared with one-dimensional simulations using full chemistry, as well as simplified one step models.

2 EXPERIMENTAL DETAILS

This section provides a brief review of the experimental setup and findings in [2]. The experiments were conducted in a shock tube with dimensions of 3400 mm $\times$ 19 mm $\times$ 203 mm, as shown in [2, 7]. The mixture studied was the H_2/O_2 mixture with an equivalence ratio of 0.5 and an initial pressure of 9 to 10 kPa at 294 K. The pressures were chosen based on the pressure limitations of the low-pressure shock tube. The cell size of the detonation at the current pressure is about 20 mm. The high-speed deflagrations were formed by passing a detonation wave through a column of equally spaced obstacles with a blockage ratio of 75%. The distance from the obstacles to the end wall is set to be 250 mm or 500 mm to have varying shock-flame complex speeds. The detonation wave thus decoupled to a shock-flame complex with a propagation speed of 48% to 54% the CJ detonation speed. The experiments for all combustion regimes discussed in the current paper were conducted at least 5 times each. The pressure evolution during the reflection was monitored by a high-frequency piezoelectric PCB pressure sensor mounted flush at the end wall of the shock tube. The pressure signals were sampled at a rate of 1.538 MHz, and low-pass filtered at 100 kHz. More details of the experiments can be found in [2].

Figure 1 compares the reflection details of the detonation and the high-speed deflagrations with detonation re-initiation, flame auto-ignition and no ignition at the end wall. The local speed of the detonation wave varies within 5% of D_{CJ}, indicating the state of the detonation wave is close to the ideal state and the loss to the channel wall is negligible. It is evident that the detonation burnt out all the reactive mixture immediately after the reflection and formed an inert shock propagating backwards to the left. The peak pressure at the end wall is about 23% larger than reflected CJ pressure (P_{refCJ}) and it decayed to P_{refCJ} in approximately $3\mu s$, as shown in Fig. 2. For the high-speed deflagration with an incoming shock speed of 54% CJ detonation speed, two auto-ignition hot spots were generated after the reflection of the leading shock, as can be seen in the second frame in Fig. 1(b). The hot spots then transited to detonation waves as shown in the third frame. From the pressure plot in Fig. 2, one can see that the reflected pressure of the leading shock is about P_{refCJ} and the re-initiation of the detonation caused a much larger pressure increase. This is almost twice the peak pressure of the reflected detonation. With a slight decrease of the high-speed deflagration speed from 54% CJ detonation speed to 48 - 49%, the distance between the leading shock and the flame becomes much larger when the shock-flame complex reached the end wall, as illustrated in Fig. 1(c-d). In Fig. 1(c), an auto-ignition spot was formed at the bottom corner near the end wall, following the reflection of the leading shock. However, the auto-ignited flame does not seem to be strong enough to accelerate to a detonation. Moreover, no significant pressure difference is noted when compared to the case with no ignition, see Fig. 2.

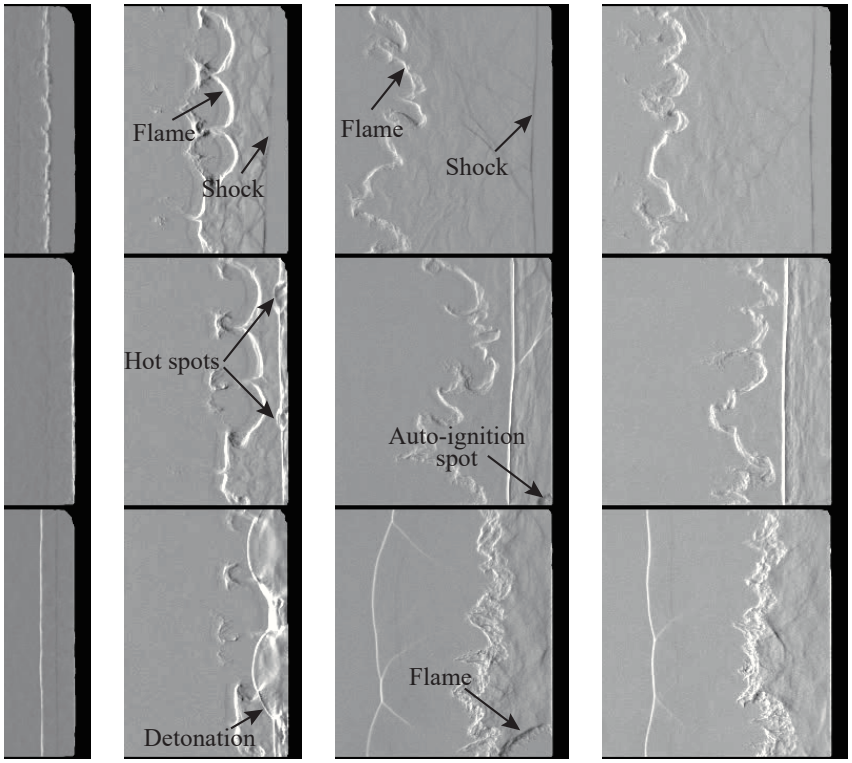

Fig. 1: Schlieren image sequence of (a) detonation reflection, and high-speed deflagration reflection with (b) detonation re-initiation, (c) flame auto-ignition and (d) no ignition at the end wall.

3 IGNITION REGIMES

Hydrogen ignition by reflected shock waves can yield different regimes of ignition e.g. the mild ignition and strong ignition [8, 9], which depends on whether the reflected shock temperature falls above or below the chain branching cross-over temperature. Near the transition, the activation energy is expected to be very high [10]. In order to interpret the thermodynamic state of the substance behind the reflected shock that caused the different ignition regimes, the activation energy $\frac{Ea}{RT_{rs}}$ and the ratio of induction to reaction time t_{ig}/t_r was calculated using the San Diego thermodynamic database [11]. Here, T_{rs}, t_{ig} and t_r are the temperature, ignition delay time and the reverse of the maximum thermicity for the gas at the post-reflected state. As exhibited in Fig. 3, the experiments with detonation re-initiation are at the chain branching cross-over regime, at which both the activation energy and the reaction intensity are high. This means that the mixtures react fast and are sensitive to fluctuations. At the state where $t_{ig}/t_r > 10^4$, the reflection of the shock forms no detonation. Whereas for a detonation wave of the current mixture, the activation energy and t_{ig}/t_r are low.

4 MODELLING APPROACHES

To study the re-initiation of detonation at the aforementioned fast reaction regime, we formulated a one-dimensional model assuming the states behind the shocks are uniform. It is addressed by the reactive Euler equation using one step and two step combustion models, and verified by the full chemistry Navier-Stokes fluid dynamics model.

The governing equations for the one step and two step combustion models are the one-dimensional reactive Euler equations, i.e., the equations of the conservation of mass, momentum, and energy in the reactive fluid, as shown in [5]. The equations were solved using a finite-volume in-house code developed by Sam Falle at the University of Leeds [12] using a second-order accurate Godunov exact

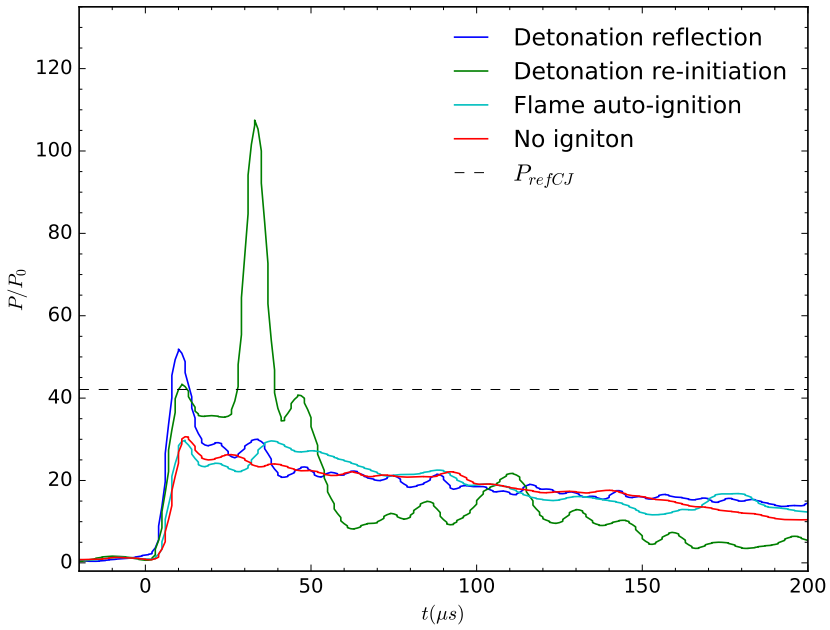

Fig. 2: Pressure profiles at the end wall recorded for the reflection of detonation and high-speed deflagration with detonation re-initiation, flame auto-ignition and no ignition.

Riemann solver [13] with adaptive mesh refinement. For the one step combustion model, the irreversible Arrhenius equation was used to describe the reaction rate, which is written as

$$\frac{D\lambda}{Dt} = K(1-\lambda)exp(-\frac{Ea}{RT}), \tag{1}$$

where λ is the reaction progress variable, $\lambda = 0$ at the shock and $\lambda = 1$ at the end of reaction. K is the pre-exponential factor evaluated so that at $\lambda = 0.5$ corresponds to one induction length (Δ_i).

In the two step chain-branching model, the ignition delay and energy deposition time can be independently controlled. The transport equations of the induction and reaction variables can be written as

$$\frac{\partial \lambda_i}{\partial t} + \frac{\partial u\lambda_i}{\partial x} = [1 - H(\lambda_i)]k_i exp(-\frac{Ea}{RT}), \tag{2}$$

$$\frac{\partial \lambda_r}{\partial t} + \frac{\partial u\lambda_r}{\partial x} = \mathcal{H}(\lambda_i)k_r(1-\lambda_r)^{0.5}, \tag{3}$$

with

$$\mathcal{H}(\lambda_i) = \begin{cases} 1 & \text{if } \lambda_i >= 1 \\ 0 & \text{if } \lambda_i < 1 \end{cases} \tag{4}$$

where λ_i is the progress variable for the induction zone with a value of 0 in the reactants and 1 at the end of the induction zone; λ_r the reaction progress variable with a value of 0 in the unburned zone and 1 in the burned products. $\mathcal{H}(\lambda_i)$ is the Heaviside function, which disables the progress of λ_i at the end of the induction zone. k_i and k_r are rate constants.

The one-dimensional full chemistry Navier–Stokes fluid dynamics model was also adopted to verify the simplified combustion model. The governing equations were solved by a 5^{th} order shock-capturing weighted essentially non-oscillatory (WENO) scheme [14] for the convective terms and an 8^{th} order central difference scheme for the diffusive terms. The Chemkin transport library was used to obtain the transport properties. A 3^{rd} order explicit Runge–Kutta scheme was used to advance the solution in time. The reaction mechanism from Burke et al. [15] involving 9 reactive species and 23 elementary reaction steps was employed. To deal with chemical stiffness, an operator splitting along with an implicit

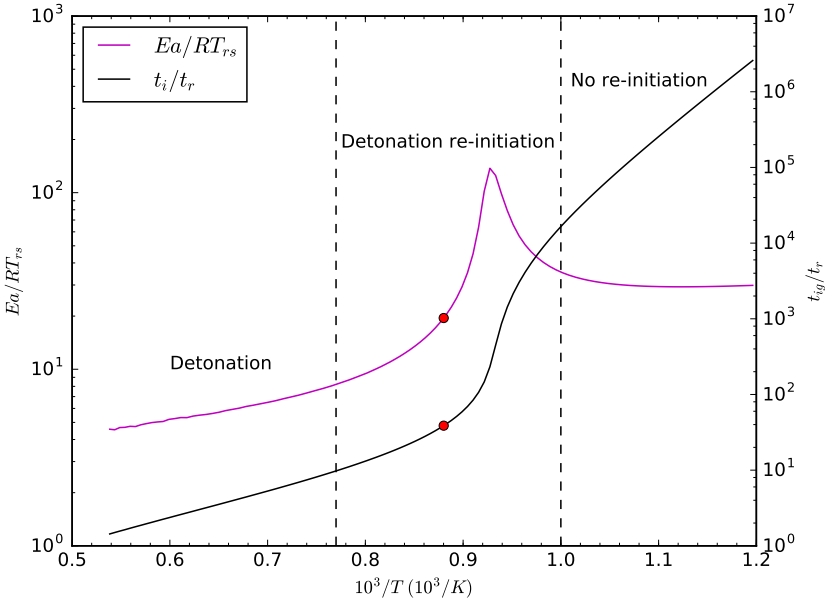

Fig. 3: The activation energy vs. the ratio of induction to reaction time for the state behind the reflected shock illustrating the chain branching nature of hydrogen.

Table 1: Model parameters for the shock induced ignition calculation.

Z_i	Mrs	$\frac{t_{ig}}{t_r}$	γ	E_a/RT_{rs}	Q/RT_{rs}	k_i	k_r	K
7.71	2.04	38.7	1.3645	19.5	4.333	2.93×10^8	32.73	1.12×10^7

Runge–Kutta method of 5^{th} order, radau5 [16] was implemented.

The input parameters for the model are given in Table 1. They were chosen to study the pressure evolution at a relatively high activation energy and high t_{ig}/t_r in the cross-over regime of the H_2/O_2 mixture. In Table 1, Z_i is the overpressure of the leading incoming shock, γ is the specific heat at the post-shock state, M_{rs} is the reflected shock Mach number and Q is the heat release. The heat release in the one step and two step combustion models were evaluated to fit the constant volume combustion pressure in the full chemistry constant volume reactor. As shown in Fig. 4, by manipulating the rate constants, both the simplified models retain the essential features of the constant volume pressure evolution obtained from full chemistry.

For simplicity, we consider a piston-driven at constant speed into the initially uniform reactive material. The piston motion will drive a shock wave into the fluid, which raises the temperature and initiates the ignition. A base grid of 500 grid points per half reaction length or induction zone length with 6 grid refinement levels is used for the 1-step model or 2-step model. In the full chemistry calculation, approximately 16 points were set in the reaction zone. The domain length was set to be long enough to capture the flow evolution for the re-initiation. A symmetric boundary condition was imposed on the left boundary, and a zero-gradient boundary condition was applied to the right side.

5 RESULTS AND DISCUSSION

5.1 Flow evolution

Here we take the result of the two step combustion model as an example to show the flow field evolution. This can be best understood by referring to the space-time diagram in Fig. 5, together with the pressure evolution in Fig. 6 and the pressure profile at the end wall in Fig. 7. The evolution of the particle paths, C^+ characteristics, the shock trajectory and the flame marked by the 90% of the consumption of reactant

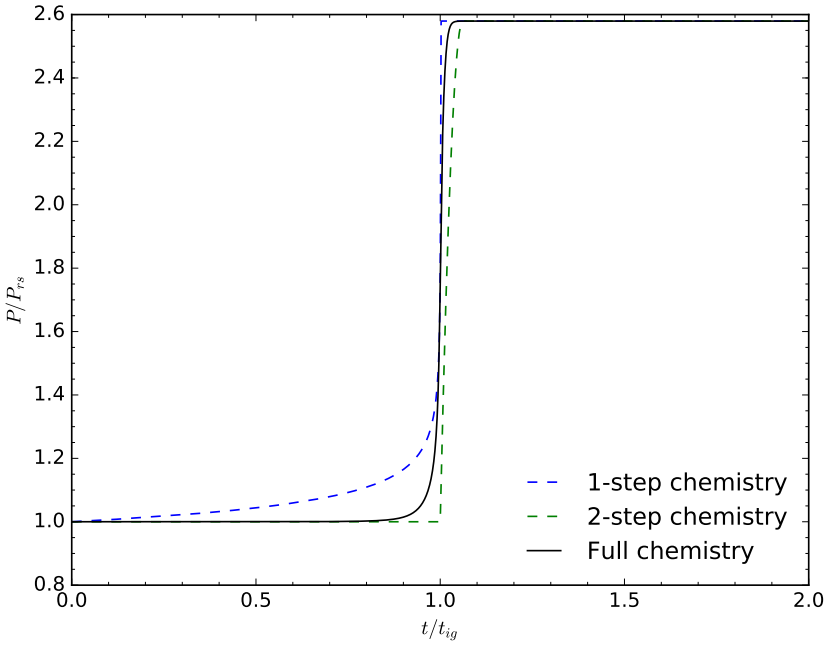

Fig. 4: Comparison of full chemistry, one step and two step combustion models by fitting constant volume combustion pressure P_{cv}.

are shown in the space-time diagram in Fig. 5. Note that $t/t_{ig} = 1.0$ in Fig. 5 marks the end of the induction and the beginning of the reaction. It seems that the pressure at the end wall went through five distinct stages during the detonation re-initiation. The first stage marks the detonation wave formation in the shocked state shortly after the onset of the reaction as the energy deposition time is much smaller than the induction time. In this stage, the end wall witnesses a sharp increase of pressure as shown in Figures 6 and 7. It lasted for about 0.1 t_{ig}. The detonation wave then becomes more steady, and the gap between the red line and the first C^+ characteristics at the top of the red line illustrates the formation of the isentropic expansion from the detonation to the end wall. In this stage, the pressure at the end wall gradually asymptotes to the peak value. The detonation wave reaches the leading shock at 1.94 t_{ig} and forms a forward-facing detonation and a series of backwards-facing waves. These waves, which are similar to the waves formed during the longitudinal oscillation in a square-wave detonation [17], in order of time sequence are an expansion wave caused by the two inert shock interaction, a compression wave formed due to the shorter ignition time of the particles at the contact discontinuity formed during the interaction of the two shocks, and lastly an expansion wave established when the old reaction front reached the newly formed reaction zone. The expansion wave formed during the interaction of the two shocks reached the end wall at 2.25 t_{ig} and the reflection of the expansion wave led to a sharp decrease of the pressure at the end wall. The end wall pressure then went through a gradual increase as the compression wave reflected back from the wall. In the last stage, the second formed detonation became steady, and the pressure at the end wall remained constant. Note that, if the simulation last for a longer time, the expansion wave will catch up with the detonation wave, and the interaction will lead to another expansion wave to come to influence the end wall pressure. However, this will happen over a much longer timescale.

Assuming a steady detonation wave at the post reflected and incoming shock, one can estimate the pressure at the end wall by assuming a Taylor wave all the way to the wall by adopting the method of characteristics. With all the C^- characteristics originating from the rear of the detonation wave, where the flow is at CJ condition, one can have the C^- characteristics:

$$J^- = \frac{2c}{\gamma - 1} - u = \frac{2c_{CJ}}{\gamma - 1} - u_{CJ} = constant. \tag{5}$$

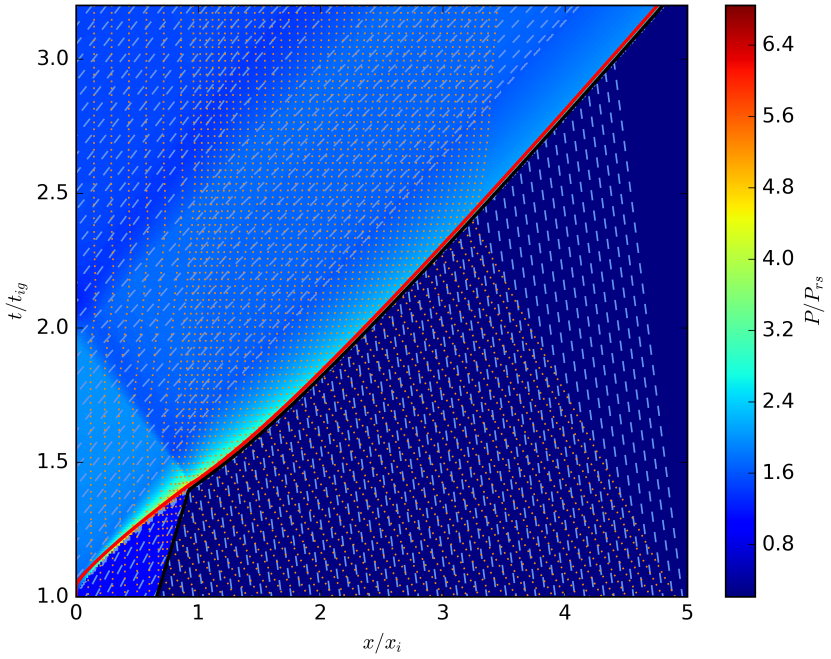

Fig. 5: Characteristic space-time on top of the pressure profile to illustrate the initiation induced by the shock reflection for one-dimensional two step simulation; the orange dotted lines represent the particle path; the light blue lines are the C^+ characteristics; the red line indicates the 90% of the consumption of reactant; the blue line is the main shock front. $x_i = t_{ig} \times \sqrt{P_{rs}/\rho_{rs}}$

At the end wall $u = 0$, one can thus get the sound speed at the end wall to be

$$c_w = c_{CJ} - \frac{\gamma - 1}{2} u_{CJ}. \tag{6}$$

Since the flow is isentropic from the CJ state all the way to the wall, we have the isentropic relations $P \propto c^{\frac{2\gamma}{\gamma-1}}$ or in terms of the CJ state:

$$\frac{P_w}{P_{CJ}} = (\frac{c_w}{c_{CJ}})^{\frac{2\gamma}{\gamma-1}}. \tag{7}$$

Assuming a first formed detonation to be strong and the reaction time is much smaller than the induction time, we can estimate the total time span of the peak pressure, which is the time from the formation of the detonation until the first formed expansion wave reached the end wall following Law [18]. The time can thus be given by

$$t_p = \frac{2L}{D_{CJ}} (\frac{\gamma + 1}{2\gamma})^{\frac{\gamma+1}{2(\gamma-1)}}, \tag{8}$$

where L in the current study is the distance between the end wall and the leading shock, the D_{CJ} is the CJ detonation speed at the post shock state.

As the reflection of the series of waves formed when the detonation catch-up with the leading shock poses a relatively small pressure difference, we can assume that the peak pressure drops to the CJ reflection pressure immediately after the first expansion reflects from the wall. We thus can formulate a square wave model to predict the pressure evolution during the initiation process. Figure 7 shows the proposed model from which p_{wref} and p_{wps} are calculated by assuming the steady detonation wave at the post reflected and incoming shock state respectively. The end wall pressure remains constant in the ignition regime before 1 t_{ig}, and the pressure increased to the peak pressure p_{wref} until 1.78 t_{ig} when

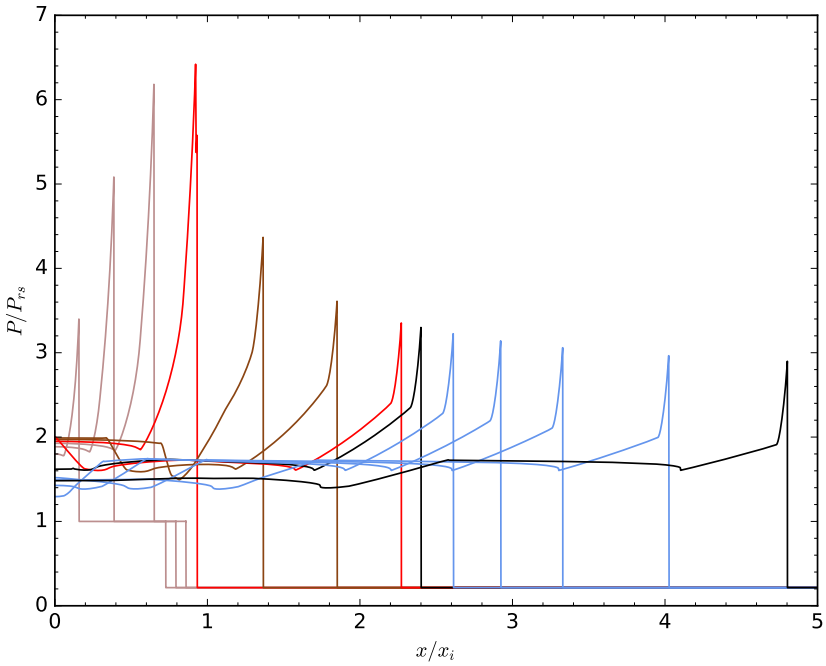

Fig. 6: Series of pressure profiles during the detonation initiation at times 1.1, 1.2, 1.3, 1.4, 1.55, 1.75, 1.94, 2.0, 2.1, 2.25, 2.45, 2.8 and 3.2 t_{ig}.

the expansion wave reaches the end wall. The pressure eventually asymptotes to the p_{wps}. As shown in Fig. 7, the simulation results seem to agree very well with the proposed model.

5.2 Comparison of the combustion models

Figure 7 compares the results of the end wall pressure in the 1D simulation using full chemistry, one step and two step combustion model. Both the simplified models agree very well with the full chemistry calculation. All three cases get the same overall evolution of the five distinct stages. The pressure evolution for the full chemistry combustion model agrees the best with the prediction, followed by the one step and two step model. This means that a simplified model can be adopted to study the problem in the limit of high reaction rate.

5.3 Influence of k_r

In the cross-over regime, the $\frac{t_{ig}}{t_r}$ is relatively high, and the energy deposition time is small. The flow disturbance can have a significant effect on $\frac{t_{ig}}{t_r}$. To study the effect of disturbances in $\frac{t_{ig}}{t_r}$, we performed numerical simulations in which k_r is varied. Figure 8 compares the pressure profile recorded at the end wall by varying k_r. For the two cases with k_r larger than the calculated value, which is 32.73, the pressure asymptotes to the maxima at an earlier time and becomes a square profile. While for the two cases with smaller k_r, the maximum pressures were much smaller than the rest cases. For the case with a k_r 10 times smaller, it seems that the first detonation was not steady before reaching the leading shock, as evidenced by the disappearance of the pressure increase stage after the expansion wave reflection.

Figure 9 compares the influence $k_r = 3.273$ and $k_r = 327.3$ on the flow fields in the space-time diagram. It is shown that the larger k_r, i.e. smaller t_r, provides a more rapid formation of steady detonation inside the shocked region followed by the Taylor wave, which is marked by the blank region behind the reaction zone. While in the low k_r flow field, with a longer reaction zone, the Taylor wave formed behind the first detonation was not able to reach the steady state when the detonation reaches the leading shock, the expansion wave thus reached the end wall at much later time.

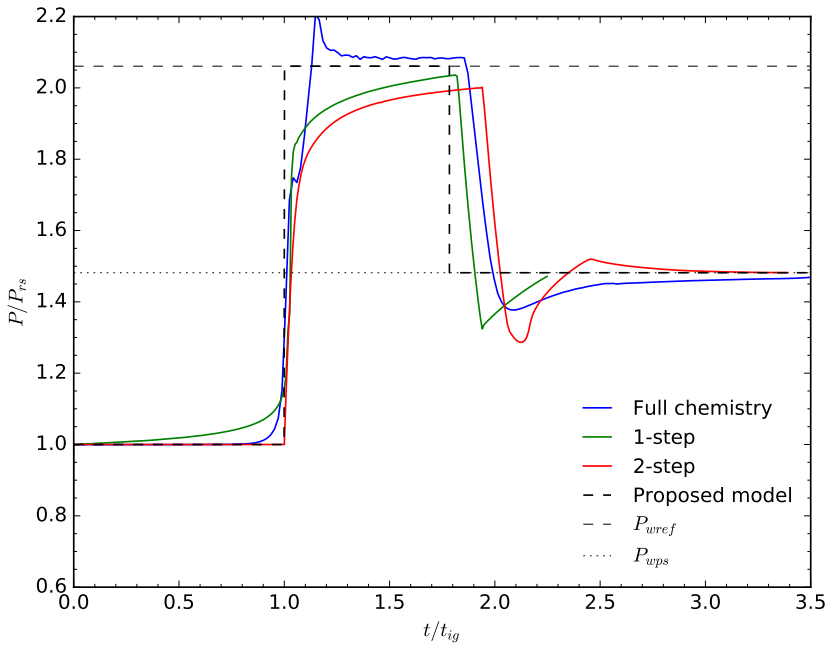

Fig. 7: Comparison of the pressure at the end wall in the one-dimensional simulation using full chemistry, one step and two step chemistry.

6 Conclusion

In conclusion, the transition of hot spots formed by the shock reflection during the head-on reflection of high-speed deflagration provides much larger pressure loadings compared to detonation reflections. By quantifying the ignition regimes of the substance behind the reflected shock in the experiments, we found that the detonation re-initiation occurred at the cross-over regime, which has a relatively large activation energy and a very short reaction characteristic time compared to the induction time. The dynamics of the pressure evolution of detonation initiation induced by shock reflection were modeled in the limit of fast reaction times as compared to the induction time. The model was sloved by the reactive Euler equation using a one step and two step combustion model, and verified by the full chemistry Navier-Stokes fluid dynamics model. Both the simplified models were able to capture the five distinct stages of the pressure evolution during the initiation and agree very well with the full chemistry simulation. The proposed model on the prediction of the pressure evolution agrees very well with the simulations in the limit of fast reaction regime. By independently control the induction and reaction time, the variation of energy release on the pressure evolution was studied using the two step model. It was found that with a large k_r, the pressure can form a square profile in the first asymptotic stage. These findings provide clarification and theoretical prediction for the dynamics of the end wall pressure caused by the shock-induced ignition.

Acknowledgments

The authors wish to thank Z. Liang from Canadian Nuclear Laboratorie and E. Studer and S. Koudriakov from Université Paris-Saclay CEA for the sponsorship and useful discussions.

References

[1] E. Studer, S. Koudriakov, D. Fernando, Detailed examination of deformations induced by internal hydrogen explosions: open questions, CEA, Personal Communication to M. Radulescu (2022).

[2] H. Yang, W. Rakotoarison, A. Sow, Z. Liang, M. Radulescu, The pressure dynamics from head-on

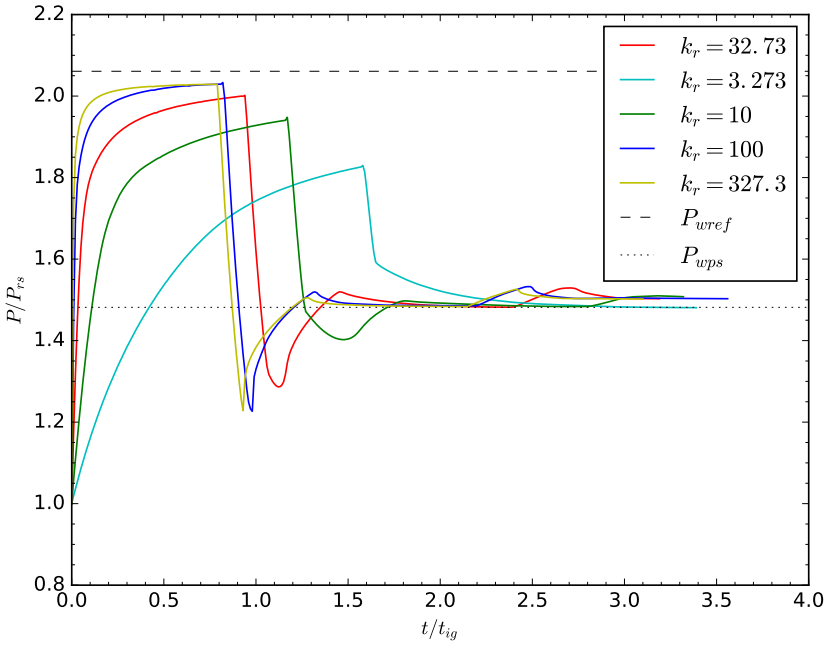

Fig. 8: Comparison for the influence of k_r on pressure at the end wall as a function of time.

reflections of detonations and high-speed deflagrations in lean hydrogen mixtures, in: Combustion Institute-Canadian Section, 2022.

[3] R. A. Strehlow, Combustion fundamentals, McGraw-Hill College, 1984.

[4] A. Kapila, D. Schwendeman, J. Quirk, T. Hawa, Mechanisms of detonation formation due to a temperature gradient, Combustion Theory and Modelling 6 (4) (2002) 553.

[5] G. J. Sharpe, Shock-induced ignition for a two-step chain-branching kinetics model, Physics of Fluids 14 (12) (2002) 4372–4388.

[6] L. Clifford, A. Milne, T. Turanyi, D. Boulton, An induction parameter model for shock-induced hydrogen combustion simulations, Combustion and flame 113 (1-2) (1998) 106–118.

[7] H. Yang, M. I. Radulescu, Enhanced DDT mechanism from shock-flame interactions in thin channels, Proceedings of the Combustion Institute 38 (3) (2021) 3481–3495.

[8] J. Meyer, A. Oppenheim, On the shock-induced ignition of explosive gases, in: Symposium (International) on Combustion, Vol. 13, Elsevier, 1971, pp. 1153–1164.

[9] H. D. Ng, Y. Ju, J. H. Lee, Assessment of detonation hazards in high-pressure hydrogen storage from chemical sensitivity analysis, International Journal of Hydrogen Energy 32 (1) (2007) 93–99.

[10] S. Browne, Z. Liang, J. Shepherd, Detailed and simplified chemical reaction mechanisms for detonation simulation, Western States Section of the Combustion Institute (Fall 2005).

[11] UCSD, Chemical-kinetic mechanisms for combustion applications, San Diego Mechanism web page, Mechanical and Aerospace Engineering (Combustion Research) (2016).

[12] B. Maxwell, A. Pekalski, M. Radulescu, Modelling of the transition of a turbulent shock-flame complex to detonation using the linear eddy model, Combustion and Flame 192 (2018) 340–357.

[13] S. Falle, J. Giddings, K. Morton, M. Baines, Numerical Methods for Fluid Dynamics 4, Clarendon Press, Oxford, 1993.

[14] C. Shu, B. Cockburn, C. Johnson, E. Tadmor, Advanced numerical approximation of nonlinear hyperbolic equations, Lecture Notes in Mathematics 1697 (1998) 325–432.

[15] M. P. Burke, M. Chaos, Y. Ju, F. L. Dryer, S. J. Klippenstein, Comprehensive H_2/O_2 kinetic model

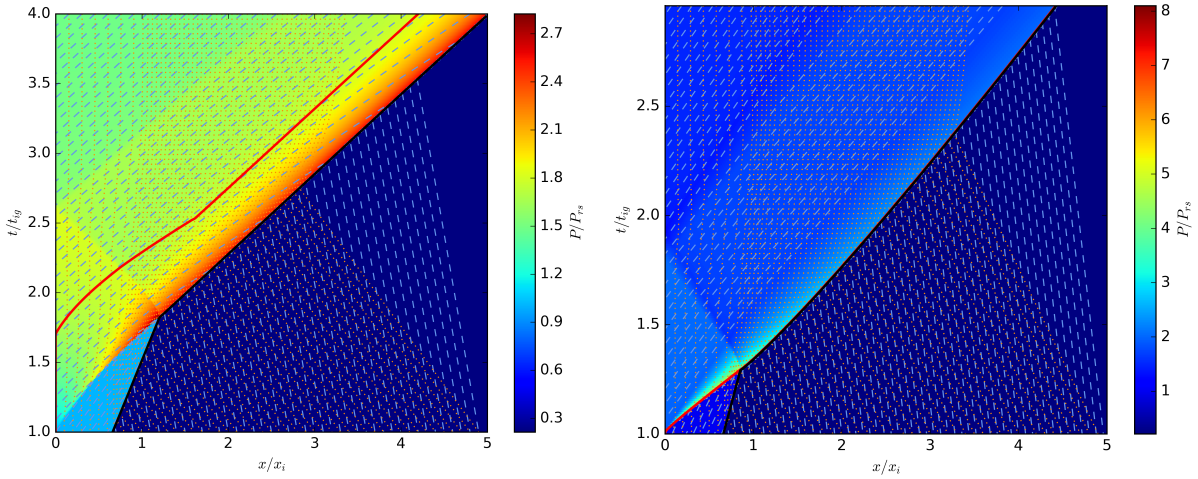

(a) (b)

Fig. 9: Comparison of (a) $k_r = 3.273$ and (b) $k_r = 327.3$ on the flow field illustrated by the space-time diagram on top of the pressure profile, same legend as for Fig. 5.

for high-pressure combustion, International Journal of Chemical Kinetics 44 (7) (2012) 444–474.

[16] E. Hairer, G. Wanner, Radau5-An implicit runge-kutta code, Report, Université de Geneve, Dept. de mathématiques, Geneve (1988).

[17] W. Fickett, W. C. Davis, Detonation: theory and experiment, Courier Corporation, 2000.

[18] C. K. Law, Combustion physics, Cambridge university press, 2010.